Robust matching in an uncertain world

Frédéric Sur

INSTITUT NATIONAL DE RECHERCHE EN INFORMATIQUE ET EN AUTOMATIQUE

Robust matching in an uncertain world

Frédéric SUR

N° 7374

September 2010

Vision, Perception and Multimedia Understanding

ISSN 0249-6399 ISRN INRIA/RR--7374--FR+ENG

INSTITUT NATIONAL
DE RECHERCHE
EN INFORMATIQUE
ET EN AUTOMATIQUE

INRIA

centre de recherche
NANCY - GRAND EST

Robust matching in an uncertain world

Frédéric SUR

Theme : Vision, Perception and Multimedia Understanding
Équipe-Projet Magrit

Rapport de recherche n° 7374 — September 2010 — 28 pages

Abstract: Finding a registration between two sets of corresponding 2D or 3D points is one of the keystones of many computer vision tasks. This is difficult since some points may not have correspondences at all, and points are often spoilt by noisy measurements. In this report we propose new robust algorithms, namely an adaptation of MSAC algorithm and a new *a contrario* model. Both of them are based on statistics over the Mahalanobis distance and explicitly take account of location uncertainty. We outline applications to SIFT keypoint matching and 3D data fusion.

Key-words: Uncertain point matching, *a contrario* model, Mahalanobis distance, SIFT keypoint matching, 3D data fusion.

Centre de recherche INRIA Nancy – Grand Est
LORIA, Technopôle de Nancy-Brabois, Campus scientifique,
615, rue du Jardin Botanique, BP 101, 54602 Villers-Lès-Nancy
Téléphone : +33 3 83 59 30 00 — Télécopie : +33 3 83 27 83 19

Appariement robuste dans un monde incertain

Résumé : L'estimation d'un recalage entre deux ensembles de points 2D ou 3D en correspondance est un des principaux problèmes rencontrés dans le domaine de la vision par ordinateur. Il s'agit d'un problème difficile car certains points peuvent n'avoir aucune correspondance dans l'autre ensemble, et la localisation des points est généralement connue à une erreur près. Dans ce report, nous proposons de nouveaux algorithmes: une adaptation de MSAC et un nouveau modèle *a contrario*. Ils sont tous deux basés sur des statistiques sur la distance de Mahalanobis et ils tiennent explicitement compte de l'incertitude dans la localisation des points. Nous suggérons des applications à l'appariement de points SIFT et à la fusion de données 3D.

Mots-clés : Appariement de points incertains, modèle *a contrario*, distance de Mahalanobis, appariements de points SIFT, fusion de données 3D.

Contents

1 Introduction

1.1 Motivation

Matching points is one of the very first steps of many computer vision tasks. The aim of matching is to find point correspondences between several (2D or possibly 3D) views of the same physical scene. As observed in [28], *matching* is not equivalent to *registration*, which consists in estimating the mapping between the aforementioned views. *Feature-based registration* (as opposed to *intensity-based registration*) refers to the estimation of the mapping, based on a set of correspondences between points of interest. Applications are for example photography stitching (see Brown and Lowe's *Autostitch* [7], Microsoft's *Photo Tourism* [33]), medical images analysis (see [28] just to cite a single paper), laser scanner registration [5], etc. Point matching is also the first step for triangulation techniques to estimate the pose of a camera and a 3D model of the scene from several views. Applications are structure from motion [15], robot localization and mapping [31], etc.

In this report we focus on point matching. This is a difficult problem because of two main reasons. First, the algorithm that extracts the points of interest is in general not fully repeatable (that is, some points are not extracted in certain views due to detection problems.) Besides, occlusions can also intervene: a small object may move across the views and hide the object of interest, or more simply the object of interest may show different sides with limited common parts if the viewpoint change is too strong. As a consequence of non-repeatability and occlusions, some points simply do not have actual correspondences in other views. The second reason that makes point matching intrinsically difficult is that point of interest location is not accurately known. When considering points of interest from images (such as SIFT keypoints [19]), even with a thorough subpixel interpolation, the accuracy is limited to 0.2 / 0.5 pixel. The accuracy of 3D points from time-of-flight depth cameras or laser scanner is also limited [1].

Once (2D or 3D) points have been extracted, one can think of point matching as a variant of point clouds registration. One of the most popular algorithm for this task (used for e.g. laser scanner registration) is certainly the *Iterative Closest Point* (ICP) algorithm [4]. ICP needs a reliable prior estimation of the mapping, then iteratively associate points by the nearest neighbor criterion and reestimate the registration mapping. Thus, ICP is not adapted if points are spoilt by spurious detections and are not accurately localized, although modern development try to overcome this difficulties (see for example [32] where outliers and measurement noise are taken into account.)

A popular way to tackle unorganized point matching is to proceed in two separated steps: 1) find out a list of putative correspondences, based on some features

(descriptors) associated with points of interest, then 2) extract from this list the largest possible subset of correspondences that are consistent with a possible registration. It is difficult to match points of interest at step 1) without introducing false correspondences (also called *outliers*, as opposed to *inliers*), that is to say correspondences between points that do not actually correspond to the same physical point. Robust algorithms (in the sense that they have to deal with outliers) are therefore called for. Most popular choice is certainly RANSAC [13] and methods derived from it. RANSAC is an iterative procedure, that is based on two steps: a) draw a minimal sample to estimate the geometry, and b) build the most consistent set of correspondences with respect to this geometry. This latter set is called *consensus set*. In the end, the "most consistent" encountered set is kept. Consistency is measured by just counting the cardinality of the consensus set (original RANSAC) or by some more sophisticated fitness measure (MSAC, MLESAC [39].) When running RANSAC-like algorithms, the users need to tune several parameters by hand, which is quite tricky. Recently, Moisan and Stival [21] have proposed a new RANSAC-like procedure in the context of stereo images. Their procedure is based on a statistical model which does not need parameter tuning. It is shown to behave as well as state-of-the-art methods with large rates of outliers. We will come back to it in Section 2.

1.2 Related work

To the best of our knowledge, the problem of taking the uncertainty of localisation into account in point matching is not fully addressed. Concerning point of interest in digital images, several recent works attempt first to characterize point uncertainty. Kanazawa and Kanatani [18] wonder whether it is really *"necessary to consider covariance matrices for image features"*, and give a mixed answer. However, they simply take the inverse of the Hessian matrix of the image grey-values (which indeed corresponds to some "flatness" measure) as an evaluation of the covariance matrix of the point of interest location, independently to the detection algorithm. On the contrary, Orguner and Gustafsson [26] explicitly derive the uncertainty of the Harris-Stephens detector [16] when considering Gaussian grey-value noise. In the same spirit, Zeisl et al. [40] estimate the location uncertainty of SIFT [19] and SURF [3] features. While Harris-Stephens detector computation is fast, it is not scale invariant. On the contrary, SIFT and SURF are invariant to scale (and rotation) change, which make them attractive methods. We will come back in Section 4 to this latter interesting approach.

Concerning 3D points coming from time-of-flight laser range finder or from depth cameras, an explicit derivation of the uncertainty of the location is presented in [1]. As a side result, they also obtain the uncertainty of the estimated surface normal vector. The derivation is obtained by propagating the manufacturer-

provided angular and radial uncertainties of the laser. Taking account of uncertainty leads to improvements in registration of clouds of points [2], especially when the point clouds come from several scans acquired with different sensor techniques and thus different resolutions / accuracies [5].

Incorporating the location uncertainty in a robust matching algorithm is the main topic of several work: from 3-D registration methods [28] to point matching under projective mapping [6, 36] or homography [25] . Location uncertainty is somehow incorporated in MLESAC [39] where inliers are assumed to be spoilt by an isotropic Gaussian perturbation and outliers are uniformly randomly distributed across images. Tordoff and Cipolla [37] elaborate on MLESAC to incorporate the uncertainty on the putative transformation. In [36] we have explicitly derived a closed-form formula for the uncertainty of the fundamental matrix estimated from the 8-point algorithm, in order to incorporate it in the aforementioned Moisan and Stival's scheme [21]. From our derivation, Raguram et al. [30] propose to speed-up RANSAC by searching for correspondences in the mapped error regions (with a fixed confidence.) Among these papers, several [6, 25, 28, 36] are based on the Mahalanobis distance [20] which follows a χ^2 distribution law when considering Gaussian random variables. All of them assume that point of interest location uncertainty is isotropic and uniform over the whole dataset. In contrast, Zeisl et al. [40] derive a non-isotropic error for SIFT and SURF keypoints, and propose proof-of-concept experiments with bundle adjustment techniques.

A summary of this work appeared in the ICPR 2010 proceedings [35].

1.3 Contribution

In this report, we assume that some prior algorithm has given a set of putative point correspondences between two views. Our aim is to build a pruning algorithm as like as RANSAC to discard false correspondences, while taking the point location uncertainty into account. We propose to extend Moisan and Stival method [21] (dedicated to point matching under epipolar constraint) to the general point correspondence problems, and to adapt it for uncertain point location. Contrary to most existing methods, we do not *a priori* assume that point uncertainty is isotropic. In particular, the proposed algorithm can be applied to the uncertainty derived from [40] (SIFT keypoints) or [1] (3D points from laser range finder.)

1.4 Organization of the report

Related work and motivation are presented in the previous Section. We explain the statistical model and the algorithm in Section 2. Section 4 is about experimental assessment. We outline applications of the proposed model to SIFT matching and 3D data fusion. We conclude with Section 5.

2 Uncertainty propagation and Mahalanobis distance

2.1 Introducing the problem

In this section, we describe the point matching problem whatever the dimensionality. We suppose that one has a list of putative correspondences, from an algorithm exploiting some feature similarity (for example similarity between SIFT features or between 3D regional point descriptors [14].) Considering a set made of N couples of d-dimensional points $(x_i, y_i)_{1 \leq i \leq N}$, the aim would be to find a registration from the x_i's to the y_i's, that is a mapping A such that $\forall i \in \{1, \ldots, N\}, y_i = Ax_i$. However data from the real world make the problem dramatically more difficult than it appears. The problem is indeed complicated by the presence of outliers among the data (i.e. points such that the mapping from x_i to y_i is not consistent with A) and uncertainty (i.e. point position is not accurately known.)

The uncertainty in point position is modeled here by a Gaussian error. The x_i's (resp. y_i's) are modeled as random variables following a Gaussian distribution function with mean $\overline{x}_i$ and covariance matrix Σ_{x_i} (resp. $\overline{y}_i$ and Σ_{y_i}.) Let us recall that covariance matrices are non-singular $d \times d$ positive matrices. Let us also note that $\overline{x}_i$ and $\overline{y}_i$ are unknown.

In the presented framework, A is a parametric mapping, which needs at least p points for its estimation. For example, in the case of planar data ($d = 2$), estimating A requires 2 points if A is a zoom+rotation (similitude) transformation, 3 points if A is a general affine transformation, and 4 points if A is a homography.

In the remainder of this section, A is a linear mapping. In the most general case, A is therefore an affine transformation. However, as we shall see in Section 2.4, it is possible to adapt the proposed method to the non-linear case via linearization. The aim of this section is to define a distance between y_i and Ax_i which takes account of the uncertainty, based on the Mahalanobis distance.

2.2 Uncertainty propagation

In this section we estimate the uncertainty of $A \cdot x$, when A is a random $d \times d$ Gaussian matrix with mean $\overline{A}$ and covariance Σ_A (which is a $d^2 \times d^2$ matrix), while x is a Gaussian random variable with mean $\overline{x}$ and covariance matrix Σ_x. Let us recall that A is estimated from p points $(x_1, \ldots x_p)$ that are Gaussian random variables with mean $\overline{x_i}$ and covariance matrix Σ_{x_i}. We shall propagate the uncertainty of these p points to A, then to $A \cdot x$.

We make use of the following classic theorem.

Proposition 1 *(propagation property) Let v be a random vector in $\mathbb{R}^d$ with mean $\overline{v}$ and covariance matrix Σ, and $f : \mathbb{R}^d \to \mathbb{R}^{d'}$ be an affine map such as $f(v) =$*

$f(\overline{v}) + F(v - \overline{v})$ (where F is a $d' \times d$ matrix.) Then $f(v)$ is a random vector in $\mathbb{R}^{d'}$ with mean $f(\overline{v})$ and covariance matrix $A\Sigma A^T$.

When f is not linear, a first order Taylor series approximate gives an estimate of the covariance matrix by replacing A by the Jacobian matrix $J(\overline{v})$ of f at $\overline{v}$. Let us recall that if we denote $f(v) = (f_1(v), \ldots, f_{d'}(v))^T$ and $v = (v_1, \ldots v_d)$, then the Jacobian matrix of g at point $\overline{v}$ is the following $d \times d'$ matrix:

$$J(\overline{v}) = \begin{pmatrix} \frac{\partial f_1}{\partial v_1}(\overline{v}) & \cdots & \frac{\partial f_1}{\partial v_d}(\overline{v}) \\ \vdots & \vdots & \vdots \\ \frac{\partial f_{d'}}{\partial v_1}(\overline{v}) & \cdots & \frac{\partial f_{d'}}{\partial v_d}(\overline{v}) \end{pmatrix}. \tag{1}$$

Remark that this propagation property is the cornerstone of most papers which aim at handling uncertainty [6, 10, 17, 25, 28, 36, 37, 40, 41]. It is also the key idea of Extended Kalman Filter [29].

In this paper, $d = d'$, i.e. the x_i's and the y_i's have the same dimensionality.

2.2.1 Uncertainty of A

Let us assume that A is estimated from p correspondences $(x_1, y_1, \ldots x_p, y_p)$.

$A = (a_{i,j})_{1 \leq i,j \leq d}$ is seen here has the column vector:

$$\left(a_{1,1}, a_{1,2}, \ldots a_{1,d}, a_{2,1}, a_{2,2}, \ldots a_{2,d} \ldots a_{d,1}, a_{d,2}, \ldots a_{d,d}\right). \tag{2}$$

The covariances of the p point couples thus propagate to A, yielding the covariance matrix of A (size $d^2 \times d^2$), which can be written as:

$$\Sigma_A = J \cdot \text{diag} \begin{pmatrix} \Sigma_{x_i} & 0 \\ 0 & \Sigma_{y_i} \end{pmatrix} \cdot J^T \tag{3}$$

where J is the $d^2 \times 2dp$ Jacobian matrix of the mapping: $(x_1, y_1, \ldots x_p, y_p) \mapsto A$ with respect to every components of every x_i.

The computation of the preceding Jacobian matrix has to be adapted to the actual algorithm that is used to estimate A from a minimal sample. With Direct Linear Transform [17], A is the solution of a Singular Value Decomposition (SVD), and J then comes from the Jacobian of the SVD which is given by [27]. In [36] we have derived a closed-form formula to estimate the uncertainty of the fundamental matrix obtained by the linear 8 point algorithm [41] and SVD. In this report, we simply estimate J by a finite-difference scheme. Note that it would be possible (and painful) to derive in a similar manner closed-form formula for each application of interest.

Remark: About the uncertainty of nearly degenerated cases... A *nearly degenerated case* is encountered when the p points that are used to estimate A are in such a position that a small displacement of one of these points yields a large change in the estimation of A. For example in the planar case, such a case arises when the $p = 2$ points used to estimate a rotation are nearly superimposed, or when the $p = 4$ points to estimate a homography are nearly co-linear. In such a situation, J has some very large coefficients, yielding a large uncertainty matrix Σ_A.

2.2.2 Uncertainty of $A \cdot x$

At a first order approximation, the product $A \cdot x$ comes with a Gaussian uncertainty, as A and x. Estimating the Jacobian of the bilinear mapping $(A, x) \mapsto A \cdot x$ is straightforward. It is the $d \times d^2 + d$ matrix:

$$\begin{pmatrix} \text{diag}(x^T, x^T \dots x^T) & A \end{pmatrix}, \tag{4}$$

where $\text{diag}(A, B, \dots Z)$ denotes the block-diagonal matrix with block matrices A, $B, \dots Z$ on its diagonal.

Assuming that A and x are uncorrelated (which holds if x is not used in estimating A), the covariance matrix of $A \cdot x$ can be derived (using Proposition 1) as the following $d \times d$ matrix:

$$\Sigma_{A \cdot x} = \text{diag}(x^T, x^T \dots, x^T) \cdot \Sigma_A \cdot \text{diag}(x^T, x^T \cdot x^T)^T + A \Sigma_x A^T. \tag{5}$$

2.3 Characterizing the quality of a matching via the Mahalanobis distance

At this point, we are in a position to define a distance between y (Gaussian process with mean $\overline{y}$, covariance matrix Σ_y) and Ax (mean $\overline{A}\overline{x}$, covariance matrix Σ_{Ax}), when x and y are in correspondence through A. Assuming $\overline{y} = \overline{A}\overline{x}$ (although each of these quantities is unknown) and independence between the random variables, $y - Ax$ has mean 0 and covariance matrix $\Sigma_y + \Sigma_{Ax}$. Assuming the random variables are Gaussian, a popular way to measure the similarity between y and Ax is to use the so-called (squared) Mahalanobis distance [20]:

$$d_M(y, Ax) = (y - Ax)^T (\Sigma_y + \Sigma_{Ax})^{-1} (y - Ax). \tag{6}$$

The Mahalanobis distance being fixed, the larger the uncertainty, the larger the point distance can be.

The random variable $d_M(y, Ax)$ follows a χ^2 law with d degrees of freedom. Indeed, let us recall that if x is a zero-mean d-dimensional Gaussian vector with covariance matrix $\Sigma = Q^T Q$, then $x^T \Sigma x = (Qx)^T Qx$ is the squared norm of the

reduced Gaussian vector Qx and thus follows a χ^2 distribution with d degrees of freedom[1].

In our framework, the independence assumption holds if (x, y) does not intervene in the estimation of A. To the best of our knowledge, such a use of Mahalanobis distance has been first studied by Pennec and Thirion [28], but a workaround was needed since in their case the hypothesized mapping A is estimated from the whole dataset.

Remark: A way to symmetrize the metric is to use:

$$d_M^s(x, y) = d_M(y, Ax) + d_M(x, A^{-1}y), \tag{7}$$

that is to say:

$$\begin{aligned} d_M^s(x, y) = &(y - Ax)^T \left(\Sigma_y + \Sigma_{Ax}\right)^{-1} (y - Ax) \\ &+(x - A^{-1}y)^T \left(\Sigma_x + \Sigma_{A^{-1}y}\right)^{-1} (x - A^{-1}y) \end{aligned} \tag{8}$$

Equation (5) gives indeed $\Sigma_{A^{-1}y}$, provided $\Sigma_{A^{-1}}$ is known. This latter covariance matrix depends on Σ_A, but this dependence depends on the way A^{-1} is estimated from A. For example, if A is a rotation matrix, then $A^{-1} = A^T$ and $\Sigma_{A^{-1}}$ is just a reordering of the coefficients of Σ_A. If A is a (linear) affine transformation, then A^{-1} is the inverse of A and $\Sigma_{A^{-1}}$ can be estimated from A via the non-linear propagation property. In this case, one just needs the Jacobian matrix of the mapping from A to A^{-1}. Since $d(A^{-1}) = -A^{-1}dAA^{-1}$ (differentiate $AA^{-1} = I_d$), one has: $\frac{\partial(A^{-1})}{\partial E_{i,j}} = -A^{-1}E_{i,j}A^{-1}$ where $E_{i,j}$ is the canonical base matrix with entries equal to 0 except in position (i, j) which is 1. If A is a homography (such as in Section 4.1.1), A^{-1} is still the inverse of A in homogeneous coordinates, but the normalisation step must be taken into account in the propagation. The same kind of argument holds if A is a fundamental matrix (Section 4.1.2): F^{-1} is proportional to F^T but the normalisation has to be considered.

Let us note that, under independence assumption, $d_M^s(x, y)$ follows a χ^2 law with $2d$ degrees of freedom.

2.4 The non-linear case

If the registration mapping A is not linear, one makes use of the Jacobian matrix J_x^A of A at a point x to propagate the covariance in Section 2.2.2, Equation (5), which becomes:

$$\Sigma_{A \cdot x} = \text{diag}(x^T, x^T \ldots, x^T) \cdot \Sigma_A \cdot \text{diag}(x^T, x^T \cdot x^T)^T + J_x^A \Sigma_x J_x^{A^T}. \tag{9}$$

The computation of J_x^A is easily tractable in the applications of Section 4.

[1] Q exists from Cholesky decomposition since Σ is a symmetric positive definite matrix.

3 Robust random sample algorithm for uncertain point matching

3.1 Mahalanobis distance and mapping uncertainty

As mentioned in the introduction, a robust sample algorithm consists in drawing minimum size samples to estimate an hypothesized mapping A, then separate remaining samples between inliers and outliers. The aim is to extract the most consistent set of inliers, whatever the measure of consistency. In this paper, we distinguish between inliers and outliers based on the Mahalanobis distance. Now, from Equations (5) and (6), one notices that, all other things being equal, $d_M(y, Ax)$ is low if the covariance matrix of the mapping A is large. There is a risk that the algorithm tends to select large sets of inliers based on a highly uncertain matrix A, corresponding to unstable configurations of the points over which A is estimated.

The authors of [28] or [32] do not encounter this problem since a good prior estimate of the registration map is first given and then refined. To the best of our knowledge, the problem has been first addressed in a recent paper by Raguram et al. [30]. They restrict their robust algorithm to mappings A with a limited uncertainty. Actually, they impose that the trace of the covariance matrix Σ_A is below a certain threshold. In a similar fashion, we impose in our algorithms that the largest eigenvalue of Σ_A and $\Sigma_{A^{-1}}$ is bounded from above (below 10.0 in Sec. 4.)

In this context, one should not directly aim at maximizing the measure of fitness of the set of inliers. The optimization is now twofolds: maximize the measure of fitness but while keeping a reasonable uncertainty over A. This prevent the search from being trapped in some degenerated cases (homography estimated from 4 pairs of aligned points for examples.)

3.2 Uncertain-MSAC

MSAC (stands for M-estimator SAmple Consensus) [39] is a slight adaptation to the classic RANSAC paradigm. Although RANSAC as well as MSAC are generic parametric model finder, we describe them in the context of registration finding. MSAC is a robust sample algorithm that consists in iterating the following stages.

1. draw a minimum sample to estimate A;
2. separate between inliers and outliers with respect to a given dissimilarity measure d and a threshold T: if $d(y_i, Ax_i) \leq T$ then (x_i, y_i) is an inlier (and conversely.)

3. associate with this hypothesis the cost

$$C = \sum_i f(x_i, y_i) \quad \text{where } f(x_i, y_i) = \begin{cases} \phi(d(y_i, Ax_i)) & \text{if } (x_i, y_i) \text{ is inlier} \\ T' & \text{otherwise} \quad (\text{with } T' \geq \phi(T)) \end{cases} \tag{10}$$

In the latter equation, ϕ is a non-decreasing function.

In the end, the consensus set is the set of inliers with the lowest cost C.

Let us recall that MSAC generalizes RANSAC since the latter simply consists in defining ϕ as a 0-1 function.

Note that in Equation (10), under independence assumption, C follows a χ^2 law with $2dN$ degrees of freedom, when N is the cardinality of the current set of inliers. $\Pr(C < c)$ is then the probability that the cost of a set of inliers is below c by chance.

In this report, we propose to call Uncertain-Msac the MSAC algorithm when d is the symmetrized squared Mahalanobis distance from Equation (8), $f(x) = x$, $T' = T$, and T is such that $\Pr(C < T) = p$, where p is a free parameter of the method. In the experiments of Section 4, $p = 10^{-5}$.

Although some heuristics enable to set some of the thresholds that intervene in MSAC, there are still touchy parameters. The following section is about a RANSAC-like parameterless algorithm based on a statistical *a contrario* model.

3.3 Uncertain AC-RANSAC

3.3.1 The *a contrario* methodology

One of the contributions of this report is to propose a solution to the robust uncertain point correspondence problem via a method based on a so-called *a contrario* model. Since the seminal paper by Desolneux, Moisan and Morel [11], these models have been the subject of a large amount of literature. The books [8] and [12] and references therein give a comprehensive account of their use in many different computer vision problems. The idea behind *a contrario* models is that independent, structure-less random features can produce structured groups only with a very small probability. As pointed out as soon as in [11], the same idea governs Stewart's MINPRAN [34] that has been proposed as a RANSAC-like method (see Torr and Murray's survey article [38] for a discussion of MINPRAN as a robust estimation method.) However, though it is rarely pointed out, it is also the underlying idea of every method that makes use of the χ^2 law to set a threshold over the squared Mahalanobis distance: the goal is to find correspondences that are unlikely under independence assumption.

In the *a contrario* methodology, a group of features is said to be *meaningful* if its probability is very low under the hypothesis $\mathcal{H}_0$ that the features are inde-

pendent. Independence assumption is a way to beat Bellman's curse of dimensionality. It makes the probability computation easy, since joint laws are simply products of marginal laws. In the statistical hypothesis testing framework, this probability is called a p-value: if it is low, then it is likely that the group of interest does not satisfy $\mathcal{H}_0$ hypothesis. There must be a better explanation than $\mathcal{H}_0$ (independence) for this group. This explanation should emphasise some common causality. Here, features are grouped because they actually correspond to the same registration mapping, in spite of location uncertainty.

3.3.2 An *a contrario* model for uncertain point matching

Let us be more specific and explain how this methodology can be specialized in the context of interest. The proposed algorithm is inspired by the AC RANSAC algorithm [21]. Although AC RANSAC just deals with consistency under epipolar constraints and does not take account of uncertainty, we still call the proposed algorithm Uncertain AC RANSAC. Let us remark that we have proposed another extension of AC RANSAC to matching simultaneous photometric and geometric constraints [22, 23, 24]. This latter work does not incorporate point uncertainty.

A candidate transformation A is first estimated from a minimal subset S made of p pairs of points. Then a fitness measure for a subset $\mathcal{S}$ of the whole set of putative correspondences containing S could be defined in many way. We investigate further two particular cases, namely:

$$d_{\max}(A, S, \mathcal{S}) = \max_{(x_i,y_i)\in\mathcal{S}} d_M^s(x_i, y_i) \tag{11}$$

or

$$d_{\text{sum}}(A, S, \mathcal{S}) = \sum_{(x_i,y_i)\in\mathcal{S}} d_M^s(x_i, y_i). \tag{12}$$

With these fitness measures at hand, we now define the null hypothesis $\mathcal{H}_0$.

Definition 1 *$\mathcal{H}_0$: x_i and y_i are independent Gaussian random variables with mean $\overline{x}_i$ and $\overline{y}_i$ and covariance matrices Σ_{x_i} and Σ_{y_i} respectively, A is an independent random mapping with mean $\overline{A}$ and covariance matrix Σ_A such that $\overline{y_i} = \overline{A}\overline{x_i}$.*

Let δ be some positive number. One computes, if k denotes the cardinality of $\mathcal{S}$:

$$\begin{aligned}
\Pr\left(d_{\max}(A, S, \mathcal{S}) \leq \delta \,|\, \mathcal{H}_0\right) &= \Pr\left(\forall\, (x_i, y_i) \in \mathcal{S}, d_M^s(x_i, y_i) \leq \delta \,|\, \mathcal{H}_0\right) &(13)\\
&= \prod_{(x_i,y_i)\in\mathcal{S}} \Pr\left(d_M^s(x_i, y_i) \leq \delta \,|\, \mathcal{H}_0\right) &(14)\\
&= \left(f_{\chi^2_{2d}}(\delta)\right)^{k-p}. &(15)
\end{aligned}$$

Indeed, Equation (13) comes from Equation (11), Equation (14) comes from independence assumption, and Equation (15) comes from the property of the Mahalanobis distance which is recalled in Section 2.3, and the fact that the value of $d_M^s(x_i, y_i)$ is deterministic (and equal to 0 up to numerical precision) for p points of $\mathcal{S}$.

In a similar way,

$$\begin{aligned} \Pr\left(d_{\text{sum}}(A, S, \mathcal{S}) \leq \delta \,|\, \mathcal{H}_0\right) &= \Pr\left(\sum_{(x_i,y_i)\in\mathcal{S}} d_M^s(x_i, y_i) \leq \delta \,|\, \mathcal{H}_0\right) \quad (16) \\ &= f_{\chi^2_{2(k-p)d}}(\delta) \quad (17) \end{aligned}$$

where $f_{\chi^2_\alpha}$ is the cumulative distribution function of the χ^2 law with α degrees of freedom. Indeed, the sum of $k-p$ independent random variables identically distributed along a χ^2 law with $2d$ degrees of freedom follows a χ^2 law with $2(k-p)d$ degrees of freedom.

Loosely speaking, both probabilities estimated how it is likely that the point set of the x_i's is sent by chance via A at a distance less than δ from the corresponding points y_i's. "By chance" means here "under independence assumption".

In the *a contrario* methodology, one does not directly deal with the probabilities but rather with the so-called *Number of False Alarms*. In what follows, $d_-(A, S, \mathcal{S})$ stands for $d_{max}(A, S, \mathcal{S})$ or $d_{sum}(A, S, \mathcal{S})$.

Definition 2 *We say that a set $\mathcal{S}$ of correspondences is ε-meaningful if there exists*

1. *a threshold δ*
2. *a mapping A evaluated with p points from $\mathcal{S}$;*

such that:

$$\textit{NFA}(S, \delta) := (N-p)\binom{k}{p}\binom{N}{k}\Pr\left(d_-(A, S, \mathcal{S}) \leq \delta \,|\, \mathcal{H}_0\right) \leq \varepsilon. \quad (18)$$

where k is the cardinality of $\mathcal{S}$ and N the total number of putative correspondences.

Since f_- is non-decreasing, one has as a corollary of this definition the following proposition.

Proposition 2 *A set $\mathcal{S}$ of correspondences is ε-meaningful if there exists a mapping A such that:*

$$\textit{NFA}(S) := (N-p)\binom{k}{p}\binom{N}{k}\Pr\left(d_-(A, S, \mathcal{S}) \leq d_-^*(A, S, \mathcal{S})\right) \leq \varepsilon \quad (19)$$

where d_-^* denotes the actual value of d_- measured over the set S.

Definition 2 is motivated by the following proposition (see [8, 12, 21]), which gives a handy meaning to the Number of False Alarms.

Proposition 3 *The expected number of ε-meaningful set under $\mathcal{H}_0$ is lower than ε.*

This proposition means that 1-meaningful groups are not likely to occur by chance, and thus are of interest. Besides, the less ε, the more meaningful the group of correspondences.

3.4 Automatic threshold setting

Equation (19) balances the trade-off between the probability and the number of possible sets of size k among the N putative correspondences. With the argument above, this enables to automatically set a threshold δ^* such that if $d_-(A, S, \mathcal{S}) < \delta^*$ then $\text{NFA}(S, \delta) < 1$. The *a contrario* model automatically adapts δ to the values of k and N.

When $d_- = d_{\text{max}}$ this threshold is simply:

$$\delta(k, N) = f^{-1}_{\chi^2_{2d}} \left(\frac{1}{\left((N-p) \binom{k}{p} \binom{N}{k} \right)^{1/(k-p)}} \right) \tag{20}$$

and when $d_- = d_{\text{sum}}$:

$$\delta(k, N) = f^{-1}_{\chi^2_{2(k-p)d}} \left(\frac{1}{(N-p) \binom{k}{p} \binom{N}{k}} \right) \tag{21}$$

with $f^{-1}_{\chi^2_\alpha}$ the inverse of the cumulative distribution function of the χ^2 with α degrees of freedom.

Let us discuss a particular representative case. Assume $d = 2$, $p = 4$, which is the case of planar homographies, see Section 4.1.1. Figure 1 shows the graphs of k vs δ ($d_- = d_{\text{max}}$) and of k vs δ/k ($d_- = d_{\text{sum}}$) when $N = 100, 200, 300, 400$. In the latter case, it is indeed sounder to normalize δ (cf Equation (12).) One can see that the larger k, the larger the threshold. Such a behaviour corresponds to what a user would do with a hand-set threshold: if the outlier rate is large, he/she would use a stricter threshold, while if the outlier rate is small (hence one can get a meaningful set of correspondences with large k), he/she would be satisfied with a looser value. The threshold value not only depends on the outlier rate, but also on the total number N of putative correspondences. All other things being equal, it is "easier" for a group of size $k \simeq N$ to be meaningful when N increases. Indeed, the larger N, the less likely it is that a group of size N is consistent with a certain

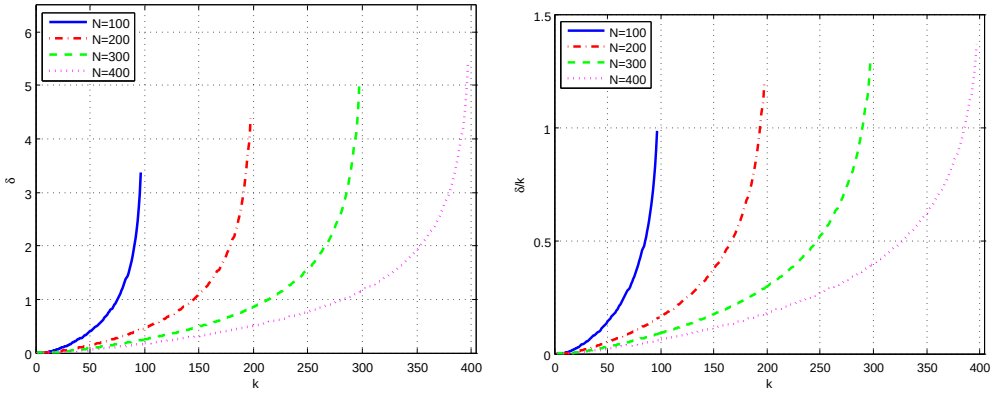

Figure 1: Largest value δ such that S is a 1-meaningful set *vs* cardinality k of S, for different values of the cardinality N of the set of putative correspondences. Left: d_{max} criterion. Right: d_{sum} criterion. The ordinate of the right graph is actually δ/k, i.e. the average Mahalanobis distance between corresponding points that belong to a 1-meaningful group of cardinality k.

distance threshold just "by chance". Comparing both d_{sum} and d_{max} criteria is not obvious, from the graphs one could feel that the sum criterion is stricter than the max one. Experiments show that in fact they give similar results.

As a comparison, let us remark that if we decide to set the threshold on the Mahalanobis distance to the usual 5% for the χ^2_2 distribution, one would get a uniform threshold value of: 0.10.

Let us discuss the meaning of the threshold on the squared Mahalanobis distance. The pixel distance between y and Ax being supposed fixed, Equation (6) show that the less uncertain y and Ax are, the larger is the squared Mahalanobis distance $d_M(y, Ax)$. Let us us do a "stress test" and assume that points are in this "worst-case" situation, and that A is the perfectly known identity transformation. For classic points of interest in images, the accuracy of the best detector may lead to $\Sigma_x = \Sigma_y = 0.5^2\text{Id}$. Thus the Euclidean norm between points in a 1-meaningful set would be (from Equation (6)): $||y - Ax||_2 < \sqrt{\delta/2}$. From Figure 1, in a set of putative correspondences spoilt by 90% of outliers, δ is between 10^{-3} ($N = 100$) and $3 \cdot 10^{-2}$ ($N = 400$.) Consequently, the *a contrario* threshold is consistent with realistic values of the Euclidean norm (around 10^{-1} pixel.)

3.5 Algorithm for *a contrario* robust matching with uncertain points

The same clever algorithm as in [21] is used.

Iterate steps 1 and 2 (2000 iterations are used in Section 4.)

1. Draw a sample S of p correspondences from the set of putative correspondences and derive the corresponding A. If the largest eigenvalue of Σ_A or $\Sigma_{A^{-1}}$ is above some threshold (10.0 in Sec. 4), then go to the next iteration.

2. Otherwise build the most meaningful subset $\mathcal{S}$ made of putative correspondences containing S by remarking (as in [21]) that when k is fixed, the subset of cardinality k with the lowest NFA is made of the k correspondences with the smallest d_M^s distances. (One thus builds nested set of correspondences.)

In the end, return $\mathcal{S}$ with the lowest NFA.

4 Possible applications

In this section, we sketch out possible applications to SIFT keypoint matching and to 3D data fusion. Of course, experimental assessment has still to be brought to completion.

4.1 Image matching

We give here applications of the proposed methodology to point of interest matching in images. We use here SIFT features [19] and we associate with each of these features the covariance matrix which quantifies the location uncertainty, as defined in [40]. The basic idea of [40] is to remark that SIFT keypoint location is defined in a scale-space approach as extrema of a Difference-Of-Gaussian pyramid $D(\mathbf{x}, \sigma)$. Since the confidence in the location is related to the "sharpness" of the extrema, the authors of [40] define the covariance matrix as proportional to the inverse of the Hessian matrix of D at the location of interest. In fact, the Hessian matrix is averaged in a vicinity of $D(\mathbf{x}, \sigma)$ to get a robust estimation. Experimental assessment in [40] demonstrate that estimating uncertainty in such a way is sound. The proportionality coefficient is defined in an *ad hoc* manner, such that the covariance matrix of circular features detected at the largest scale have Frobenius norm equal to 1. Since we judge that this leads to an overestimation of the location uncertainty (cf Figure 2), we decide to reduce it by uniformly dividing it by a 10 factor.

4.1.1 Uncertain point matching under homography constraint

We consider here planar homographies, hence $d = 2$ and $p = 4$.

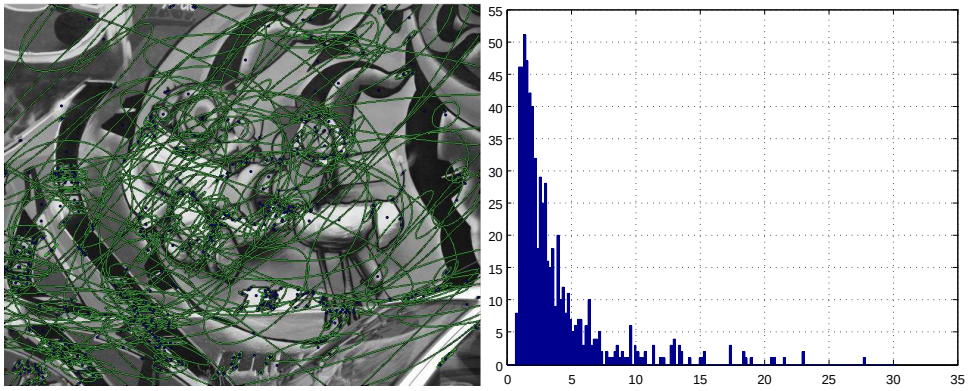

Figure 2: Zeisl et al. [40] uncertainty for SIFT points location. On the left: example of elliptical error region for SIFT extraction over an image from the Oxford's Graffiti dataset (from `www.featurespace.org`.) On the right: histogram of the square root of the determinant of the covariance matrices (geometric mean of the eigenvalues.) Compared to the commonly acknowledge average 0.5 pixel error, the uncertainty seems to us overestimated.

The set of putative correspondences is obtained by matching SIFT descriptors with the standard criterion: the nearest neighbour in the second image is matched to a SIFT descriptor from the first image provided the ratio of the distances between this nearest neighbour and the second nearest neighbour is below a certain threshold. We set here this threshold to 0.9, yielding lots of spurious putative correspondences, which makes the subsequent robust matching step more challenging. This threshold is usually set to a more conservative value (0.6-0.7.)

In the first experiment, two views of a corridor are matched. Figure 3 shows the aforementioned 44 putative correspondences. Many wrongly associated points can actually be seen. Figure 4 shows a typical result of Uncertain MSAC (Section 3.2) and Uncertain AC-RANSAC (Section 3.3.) Uncertain MSAC retrieves 12 correspondences, and 10 for Uncertain AC-RANSAC. Correspondences are found between points from the dominant plane, since a homography constraint is enforced. Results are shown with the covariances $\Sigma_y + \Sigma_{Ax}$ and $\Sigma_x + \Sigma_{A^{-1}y}$ (90% confidence ellipsoid, yellow) superimposed to the points of interest. One can see that taking the Mahalanobis distance into account automatically adapts the inlier/outlier threshold: it is gentler for points with higher uncertainty (e.g. because they are distant from the 4 points estimating A - in red.) For example, top-right point of interest in Fig. 4 (Uncertain AC-RANSAC) would not have been matched with classic RANSAC, because the distance between the point of interest (yellow) and the projection of its corresponding point via the homography A

(end of the blue line) is 40 pixels, which is larger than any reasonable threshold in classic RANSAC. This observation justifies the approach by Raguram et al. [30]: when randomly sampling the 4 points in RANSAC, some correspondences lying far away from these basis points can be classified as outliers. Thus, relaxing the distance threshold based on the uncertainty permits to speed-up the search for a large set of inliers.

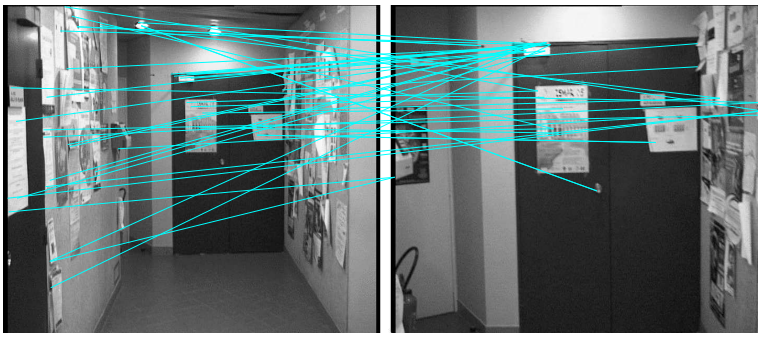

Figure 3: *Corridor* experiment. The 44 putative correspondences.

In the second experiment, two views of Notre-Dame cathedral are compared. The set of the 160 putative correspondences is in Figure 5, the outlier rate is quite large. The algorithm is run twice: once the set with the lowest NFA has been found, the algorithm is run on the whole set of correspondences minus the first group. Both groups (consistent with a homography) correspond to aligned planes. (The cathedral and the building frontage are actually aligned, which explains the matches in the 2nd group.)

4.1.2 Set of points consistent to epipolar geometry

It is a well known fact [17] that, considering an epipolar line as a Gaussian random process with mean l and covariance matrix Σ_l, then, with probability p realizations of the process lie within the hyperbola $C = ll^T - k^2\Sigma_l$ where $k = F^{-1}(p)$ and F is the cumulative distribution function of the χ^2 law with two degrees of freedom.

In [36], we have proposed to use $d(x, F \cdot y) = k^2(x)$ as a point/line distance, where x lies on the conic $C = ll^T - k^2(x)\Sigma_l$ (with $l = F \cdot y$ and Σ_l the covariance matrix of l) The covariance matrix Σ_l is obtained after a careful derivation based on the assumption that points on which fundamental matrix and epipolar lines are estimated have a location that comes with a Gaussian noise. The point/line distance was plugged in the same *a contrario* model as here. Covariance matrices for fundamental matrix and epipolar lines was first derived in [10] (see also [17] and

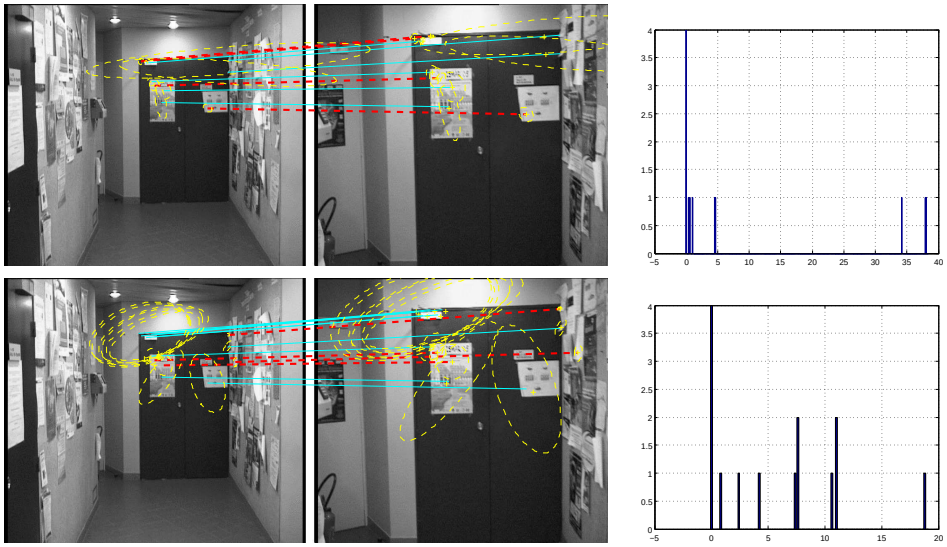

Figure 4: *Corridor* experiment. Top: Uncertain AC-RANSAC. 10 correspondences are retrieved. Bottom: Uncertain MSAC. 12 correspondences are retrieved. On the right, histograms of the Euclidean distance between the points of interest from the second image (yellow crosses) and the projection of the points from the first image (ends of the blue lines.) One can see that both algorithms may lead to select inliers with large Euclidean distances. Of course, such inliers would not have been considered as inliers with standard RANSAC.

Figure 5: *Notre-Dame* experiment. The 160 putative correspondences.

references therein.) Seeking points along epipolar line based on the uncertainty was also achieved in [6]. We do not elaborate further on this aspect in this report.

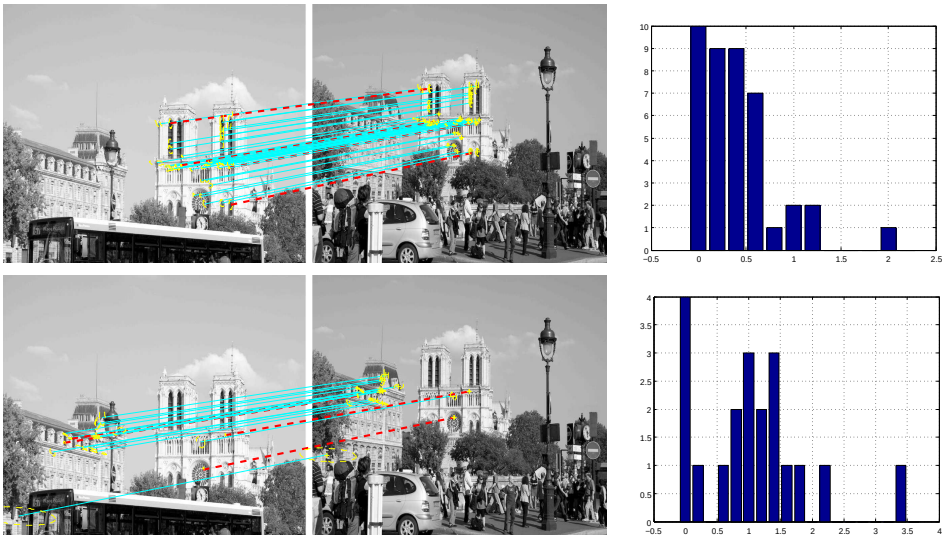

Figure 6: *Notre-Dame* experiment. Top: most meaningful set of correspondences from Uncertain AC-RANSAC (41 matches.) All points lie on the façade of the cathedral. Bottom: most meaningful set when discarding the previous correspondences from the 160 putative correspondences (20 matches.) The building in the foreground is actually aligned with a part of the cathedral. On the right: Euclidean distance histograms.

4.2 3D point correspondences under homography constraint

We propose here an experiment about 3D data fusion based on synthetic data. The aim is to identify the 3D homography between two clouds of matched points, which contain outliers. A possible application could be registration from depth cameras or laser range finder data as in [1]. Propagating the uncertainty of the range camera measurements to the 3D points could indeed provide valuable information for partially overlapping reconstructions as in [5]. Let us remark that the literature about 3D registration is mainly based on variants of ICP [4]. In our framework based on a set of putative correspondences, one could image drawing correspondences from the so-called *regional point descriptors* and especially from the 3D shape context [14].

Experimental setting. 1,000 points are uniformly drawn in a $100 \times 100 \times 100$ block, and separated between inliers (I) and outliers (O). Inliers x_i are transformed by a 3D homography into the y_i, and outliers are associated with uniformly drawn points into the 3D area limited by the inliers. Each point is associated with a random covariance which may have standard deviation up to 6 in a direction, and

its position is changed with a standard deviation of 3 (compare to the size of the block: the problem is quite challenging.)

The table 1 gives statistics for the Uncertain AC-RANSAC algorithm (average over 10 runs) in 10 situations. *"# inliers"* and *"# outliers"* are respectively the number of inliers and the number of outliers among the $1,000$ correspondences in each experiment; *"# retrieved"* is the number of points in the most meaningful group returned by the algorithm; *"# outliers among retrieved"* is the number of outliers that this group contains; *"first iteration without outliers"* is the number of iterations after which the most meaningful group encountered contains no outlier; *"# retrieved @ 1st 1-meaningful"* is the cardinality of the first 1-meaningful group; and *"# outliers @ 1st 1-meaningful"* is the number of outliers that this group contains.

While the algorithm misses a large amount of inliers, the number of outliers among the retrieved correspondences is excellent, even with large rate of outliers in the dataset. Interestingly, if one stops the algorithm as soon as a 1-meaningful group is retrieved (this is sound because of prop. 3), the retrieved group has about 20-30 correspondences and is returned on average after less than 4 iterations (up to 50% outlier rate.) This makes us expect possible speeding up of RANSAC as in [30] by stopping the Uncertain AC-RANSAC as soon as a 1-meaningful group has been retrieved, then switching to some localized RANSAC strategy [9].

# inliers	# outliers	# retrieved	# outliers among retrieved	first iteration without outliers	# retrieved @ 1st 1-meaningful	# outliers @ 1st 1-meaningful
1000	0	154.8	0	1.1	29.3	0
900	100	122.7	1.4	1.2	29.0	0.6
800	200	96.1	1.4	1.2	21.5	1.5
700	300	89.3	1.6	1.3	19.9	2.2
600	400	77.8	3.5	1.3	18.7	2.4
500	500	61.8	4.5	2.0	23.1	2.8
400	600	46.8	5.9	2.3	27.2	6.0
300	700	45.5	6.9	5.1	16.6	5.2
200	800	30.7	8.3	5.5	15.7	9.0
100	900	27.5	17.5	6.9	15.4	12.1

Table 1: *3D point correspondences*. Experiment on synthetic data.

5 Conclusion

In this report we have presented a new *a contrario* RANSAC algorithm that incorporates the uncertainty of the location of the points of interest, either in 2D or in 3D. We have also suggested experiments that outline the interest of this approach.

References

[1] K.-H. Bae, D. Belton, and D.D. Lichti. A closed-form expression of the positional uncertainty for 3d point clouds. *IEEE Transactions on Pattern Analysis and Machine Intelligence*, 31:577–590, 2009.

[2] K.-H. Bae and D.D. Lichti. A method for automated registration of unorganised point clouds. *ISPRS Journal of Photogrammetry and Remote Sensing*, 63(1):36–54, 2008.

[3] H. Bay, A. Ess, T. Tuytelaars, and L. Van Gool. Speeded-Up Robust Features (SURF). *Computer Vision and Image Understanding*, 110(3):346–359, 2008.

[4] P. Besl and N. McKay. A method for registration of 3-d shapes. *IEEE Transactions on Pattern Analysis and Machine Intelligence*, 14(2):239–256, 1992.

[5] G. Boström, J.G.M. Gonçalves, and V. Sequeira. Controlled 3D data fusion using error-bounds. *ISPRS Journal of Photogrammetry and Remote Sensing*, 63(1):55–67, 2008.

[6] S. Brandt. On the probabilistic epipolar geometry. *Image and Vision Computing*, 26(3):405–414, 2006.

[7] M. Brown and D.G. Lowe. Automatic panoramic image stitching using invariant features. *International Journal of Computer Vision*, 74(1):59–73, 2007.

[8] F. Cao, J.L. Lisani, J.-M. Morel, P. Musé, and F. Sur. *A theory of shape identification*. Number 1948 in Lecture Notes in Mathematics. Springer, 2008.

[9] O. Chum, J. Matas, and J.V. Kittler. Locally Optimized RANSAC. In *Proceedings of the DAGM Symposium*, pages 236–243, Magdeburg, Germany, 2003.

[10] G. Csurka, C. Zeller, Z. Zhang, and O. Faugeras. Characterizing the uncertainty of the fundamental matrix. *Computer Vision and Image Understanding*, 68(1):18–36, 1997.

[11] A. Desolneux, L. Moisan, and J.-M. Morel. Meaningful alignments. *International Journal of Computer Vision*, 40(1):7–23, 2000.

[12] A. Desolneux, L. Moisan, and J.-M. Morel. *From Gestalt theory to image analysis: a probabilistic approach*. Interdisciplinary applied mathematics. Springer, 2008.

[13] M. Fischler and R. Bolles. Random sample consensus: A paradigm for model fitting with applications to image analysis and automated cartography. *Communications of the ACM*, 24(6):381–395, 1981.

[14] A. Frome, D. Huber, R. Kolluri, T. Bülow, and J. Malik. Recognizing objects in range data using regional point descriptors. In *Proceedings of the European Conference on Computer Vision (ECCV)*, volume 3023, pages 224–237, Prague, Czech Republic, 2004.

[15] I. Gordon and D.G. Lowe. Scene modelling, recognition and tracking with invariant image features. In *Proceedings of the International Symposium on Mixed and Augmented Reality (ISMAR)*, pages 110–119, Arlington, VA, USA, 2004.

[16] C. Harris and M. Stephens. A combined corner and edge detector. In *Proceedings of the Alvey Vision Conference*, pages 147–151, Manchester, UK, 1988.

[17] R. Hartley and A. Zisserman. *Multiple View Geometry in Computer Vision*. Cambridge University Press, 2000.

[18] Y. Kanazawa and K. Kanatani. Do we really have to consider covariance matrices for image features? *Proceedings of the IEEE International Conference on Computer Vision (ICCV)*, 2:301–306, 2001.

[19] D. Lowe. Distinctive image features from scale-invariant keypoints. *International Journal of Computer Vision*, 60(2):91–110, 2004.

[20] P.C. Mahalanobis. On the generalised distance in statistics. *Proceedings of the National Institute of Sciences of India*, 2(1):49–55, 1936.

[21] L. Moisan and B. Stival. A probabilistic criterion to detect rigid point matches between two images and estimate the fundamental matrix. *International Journal of Computer Vision*, 57(3):201–218, 2004.

[22] N. Noury, F. Sur, and M.-O. Berger. Fundamental matrix estimation without prior match. In *Proceedings of the IEEE International Conference on Image Processing (ICIP)*, volume 1, pages 513–516, San Antonio, TX, USA, 2007.

[23] N. Noury, F. Sur, and M.-O. Berger. Determining point correspondences between two views under geometric constraint and photometric consistency. Research Report 7246, INRIA, 2010.

[24] N. Noury, F. Sur, and M.-O. Berger. Modèle a contrario pour la mise en correspondance robuste sous contraintes épipolaires et photométriques. In *Actes du congrès Reconnaissance des Formes et Intelligence Artificielle (RFIA)*, Caen (France), 2010.

[25] B. Ochoa and S. Belongie. Covariance propagation for guided matching. In *Proceedings of the Workshop on Statistical Methods in Multi-Image and Video Processing (SMVP)*, Graz, Austria, 2006.

[26] U. Orguner and F. Gustafsson. Statistical characteristics of harris corner detector. In *Proceedings of IEEE Workshop on Statistical Signal Processing (SSP)*, pages 571–575, Madison, WI, USA, 2007.

[27] T. Papadopoulo and M.I.A. Lourakis. Estimating the Jacobian of the Singular Value Decomposition: theory and applications. In *Proceedings of the European Conference on Computer Vision (ECCV)*, volume 1, pages 554–570, London, UK, 2000.

[28] X. Pennec and J.-Ph. Thirion. A framework for uncertainty and validation of 3D registration methods based on points and frames. *International Journal of Computer Vision*, 25(3):203–229, 1997.

[29] B. Quine, J. Uhlmann, and H. Durrant-Whyte. Implicit Jacobian for linearised state estimation in nonlinear systems. In *Proceedings of the American Control Conference*, volume 3, pages 1645–1646, Seattle, WA, USA, 1995.

[30] R. Raguram, J.-M. Frahm, and M. Pollefeys. Exploiting uncertainty in random sample consensus. In *Proceedings of the IEEE International Conference on Computer Vision (ICCV)*, pages 2074–2081, Kyoto, Japan, 2009.

[31] S. Se, D.G. Lowe, and J.J. Little. Vision-based global localization and mapping for mobile robots. *IEEE Transactions on Robotics*, 21(3):364–375, 2005.

[32] A. Segal, D. Haehnel, and S. Thrun. Generalized-ICP. In *Proceedings of Robotics: Science and Systems (RSS)*, Seattle, WA, USA, 2009.

[33] N. Snavely, S. M. Seitz, and R. Szeliski. Modeling the world from internet photo collections. *International Journal of Computer Vision*, 80(2):189–210, 2008.

[34] C.V. Stewart. MINPRAN: a new robust estimator for computer vision. *IEEE Transaction on Pattern Analysis and Machine Intelligence*, 17(10):925–938, 1995.

[35] F. Sur. Robust matching in an uncertain world. In *Proceedings of the International Conference on Pattern Recognition (ICPR)*, Istanbul, Turkey, 2010.

[36] F. Sur, N. Noury, and M.-O. Berger. Computing the uncertainty of the 8 point algorithm for fundamental matrix estimation. In *Proceedings of the British Machine Vision Conference (BMVC)*, volume 2, pages 965–974, Leeds, UK, 2008.

[37] B.J. Tordoff and R. Cipolla. Uncertain RanSaC. In *Proceedings of the IAPR Workshop on Machine Vision Applications (MVA)*, Tsukaba, Japan, 2005.

[38] P. Torr and D. W. Murray. The development and comparison of robust methods for estimating the fundamental matrix. *International Journal of Computer Vision*, 24(3):271–300, 1997.

[39] P. Torr and A. Zisserman. MLESAC: A new robust estimator with application to estimating image geometry. *Computer Vision and Image Understanding*, 78:138–156, 2000.

[40] B. Zeisl, P. Georgel, F. Schweiger, E. Steinbach, and N. Navab. Estimation of location uncertainty for scale invariant feature points. In *Proceedings of the British Machine Vision Conference (BMVC)*, London, UK, 2009.

[41] Z. Zhang. Determining the epipolar geometry and its uncertainty: a review. *International Journal of Computer Vision*, 27(2):161–195, 1998.

Centre de recherche INRIA Nancy – Grand Est
LORIA, Technopôle de Nancy-Brabois - Campus scientifique
615, rue du Jardin Botanique - BP 101 - 54602 Villers-lès-Nancy Cedex (France)

Centre de recherche INRIA Bordeaux – Sud Ouest : Domaine Universitaire - 351, cours de la Libération - 33405 Talence Cedex
Centre de recherche INRIA Grenoble – Rhône-Alpes : 655, avenue de l'Europe - 38334 Montbonnot Saint-Ismier
Centre de recherche INRIA Lille – Nord Europe : Parc Scientifique de la Haute Borne - 40, avenue Halley - 59650 Villeneuve d'Ascq
Centre de recherche INRIA Paris – Rocquencourt : Domaine de Voluceau - Rocquencourt - BP 105 - 78153 Le Chesnay Cedex
Centre de recherche INRIA Rennes – Bretagne Atlantique : IRISA, Campus universitaire de Beaulieu - 35042 Rennes Cedex
Centre de recherche INRIA Saclay – Île-de-France : Parc Orsay Université - ZAC des Vignes : 4, rue Jacques Monod - 91893 Orsay Cedex
Centre de recherche INRIA Sophia Antipolis – Méditerranée : 2004, route des Lucioles - BP 93 - 06902 Sophia Antipolis Cedex

Éditeur
INRIA - Domaine de Voluceau - Rocquencourt, BP 105 - 78153 Le Chesnay Cedex (France)
http://www.inria.fr
ISSN 0249-6399